Onshore preprocessing: (1) reference wave removal including ground roll and deghosting, and (2) achieving that objective with a reduced data requirement

Jing Wu and Arthur B. Weglein, M-OSRP, University of Houston

Abstract

The elastic Green's theorem wave separation method can effectively reduce ground roll and ghosts of land data, and most importantly, without harming reflection data. Both multicomponent traction and multicomponent displacement are assumed in the original elastic Green's theorem based algorithm (Wu and Weglein, 2015a). Traction can be determined in terms of derivatives of displacement and local earth properties in the vicinity of acquisition surface. In order to reduce the requirement of determining traction, this paper simplifies the algorithm by assuming that the acquisition is performed on a vacuum/earth interface. With that assumption, the requirement of traction is reduced by asking for an approximate source wavelet or the external force information at source point. Synthetic data tests show very useful and acceptable results using the vacuum/earth assumption when the input data are generated from an air/earth model, which is more realistic.

1 Introduction

Onshore seismic exploration and processing seek to use reflection data (the scattered wavefield) to make inferences about the subsurface information. However, besides the reflection data, the measured total wavefield also contains direct wave and surface wave (also called ground roll), which can interfere with reflections. As a main type of coherent noises, ground roll dominates the energy of measured data, and it can seriously mask the reflections. Therefore, ground roll removal is an essential processing step for onshore application. The current ground roll removal methods, e.g., filtering methods in the frequency-wavenumber (ω, k_x) domain or the frequency-offset (ω, x) domain (Yilmaz, 2001), may damage the reflection

data, especially when ground roll interferes with the reflection. In addition, in the case of buried sources or buried receivers, not only are there upgoing waves in the reflection data, there are also ghosts, which correspond to the downward reflection at air/earth boundary. On one hand, ghosts can cause notches starting at very low frequencies if measurements are deep beneath the air/earth surface; on the other hand, they can seriously interfere with the up waves when the measurement surface is close to the air/earth surface. The upgoing reflected waves are usually pursued for subsequent processing. In this paper, we will discuss both the ground roll removal and deghosting problems.

As a flexible and useful tool, Green's theorem provides a method to achieve these two goals – removal of the ground roll and removal of the ghosts, without damaging the upgoing reflection data. The distinct advantages of applying the wave-separation method based on Green's theorem have been demonstrated by Weglein et al. (2002); Zhang (2007); Mayhan and Weglein (2013); Tang et al. (2013); Yang et al. (2013). The application of this method is mature for marine exploration. In a further step, we have extended this method to accommodate the elastic land data, where ground roll becomes a key issue (Wu and Weglein, 2014; 2015a;b).

For onshore plays, the extended elastic Green's theorem method is applicable for displacement data (Pao and Varatharajulu, 1976; Weglein and Secrest, 1990; Wu and Weglein, 2015a). Both the ground roll and the receiver-side ghosts can be removed in one step, when a homogeneous elastic whole space is chosen as the reference medium. However, the method demands the multicomponent traction and multicomponent displacement as input, in which the traction is not directly available in general. This requirement limits the practical application of this method.

In this paper, we get rid of the reliance on traction for wider application of this method in practice. The original formula can be modified to call for the approximate source wavelet information instead of traction at all the points along the acquisition surface, by assuming (1) the world to be a half space of vacuum over a half space of earth, (2) the external force acting on the vacuum/earth boundary is local, and (3) the acquisition is right beneath the vacuum/earth boundary.

A numerical test is designed to examine the usefulness of the vacuum/earth assumption and the corresponding simplified wave separation algorithm. The input data to the simplified algorithm is generated from a half space of air over a half space of elastic earth, but the method processes such data as though it was from a vacuum/earth world. It produces a

positive result that removes majority energy of ground rolls and ghosts, and meanwhile retains the upgoing reflection data. The method we provide in this paper make the current onshore acquisition be able to benefit from the Green's theorem based wave separation method for ground roll removal without needing traction any more, and provides practical values.

2 Elastic Green's theorem wave separation theory

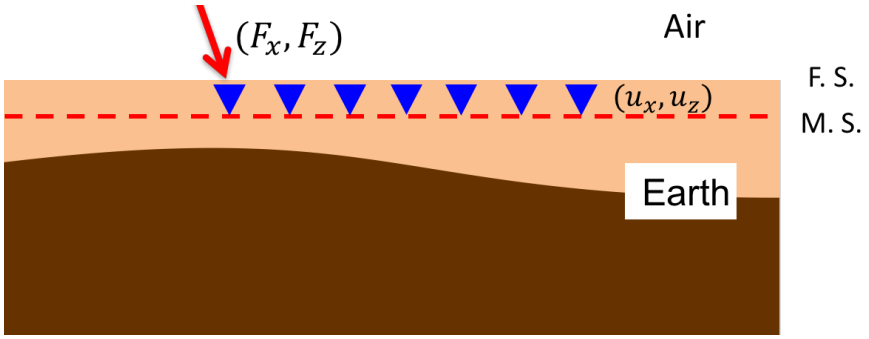

Figure 1: A generic model describing the onshore experiment. The blue triangles represent the receivers. F.S. for the free surface, or the air/earth boundary; M.S. for the measurement surface.

Figure 1 shows a generic onshore model consisting of an air half-space and an elastic-earth half-space. Receivers are buried in the earth, and source (e.g., vibroseis) in the form of a force is applied on the free surface (F. S.). Therefore, ghosts exist at the receiver side only. The measurement surface (M. S.) can be close to the free surface as in the case of on-surface-receiver acquisition; it can be also meters below the free surface for buried receivers. However, the receivers are coupled with the elastic medium for both situations. Assuming that the portion of earth along the measurement surface is homogeneous and known, the reference medium can be chosen as a homogenous elastic whole space (Figure 2), whose property agrees with the actual earth along the measurement surface.

There are three sources (Figure 3) acting on the selected homogeneous reference medium: the energy source (the force S_1), and two passive sources (the perturbations S_2 and S_3). S_1 and S_2 collaborate to produce the ground rolls, the direct wave and the receiver ghosts. S_3 generates upgoing reflection from the earth. The upgoing waves due to S_3 are expected to be separated out from those produced by both S_1 and S_2. Choosing a closed semi-infinite

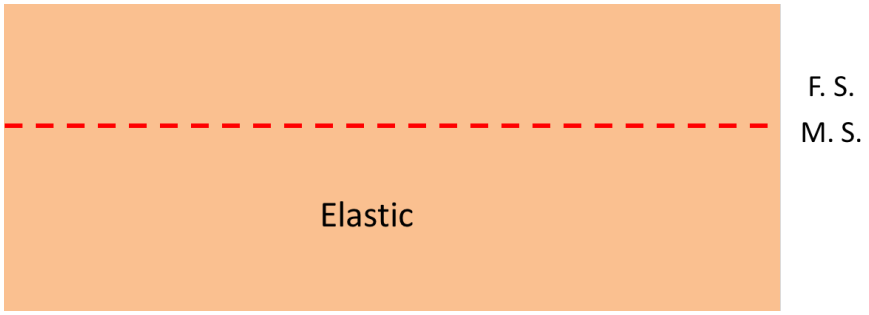

Figure 2: A homogeneous whole-space reference medium, agrees with the actual earth along the M.S.

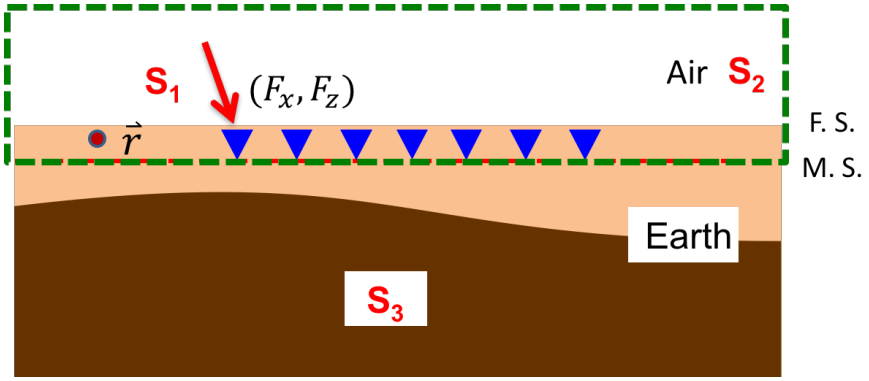

Figure 3: Three sources act on the reference medium, and the surface integral along the dashed green line extracts the contributions from S_3, for evaluation point $\vec{r}$ inside the volume. With respect to the reference medium, S_1 for energy source, S_2 for air perturbation, and S_3 for earth perturbation.

surface bounded below by the measurement surface, and evaluating the surface integration inside the volume, then the portion of the wavefield due to the source outside the volume can be produced; i.e., the contribution of S_3, which is the upgoing wave, can be predicted inside the volume.

The Green's theorem wave separation formula is

$$\begin{aligned} &\vec{u}^{up}(\vec{r},\omega) \\ &= -\int_{m.s.} [\vec{t}(\vec{r}',\omega)\cdot\mathbf{G}_0(\vec{r}',\vec{r},\omega) - \vec{u}(\vec{r}',\omega)\cdot(\hat{n}\cdot\mathbf{\Sigma}_0(\vec{r}',\vec{r},\omega))]d\vec{r}', \end{aligned} \tag{1}$$

where $\vec{r}'$ is the receiver point, $\vec{r}$ is the evaluation point, $\vec{u}$ is the displacement, and $\vec{t}$ is the traction along the measurement surface; $\mathbf{G}_0$ is the Green's displacement tensor, $\mathbf{\Sigma}_0$ is the

Green's stress tensor; $\vec{u}^{up}$ is the predicted upgoing wave. $\hat{n}$ is the normal outside vector along the measurement surface; ω is the radial frequency; and $\cdot$ represents a tensor product.

By applying Equation 1, we can remove ground rolls, direct waves, and ghosts simultaneously. There are three important points with respect to Equation 1: (1) No source information is required, neither amplitude nor radiation pattern. (2) The integrals are carried out at receiver side only and work on one experiment at a time, resulting in relatively small data requirement and low computational cost. (3) There is no assumption about the shape of the measurement surface – it can be flat, inclined, or undulating.

3 Formula simplification

Equation 1 calls for both the multicomponent displacements and traction. We derive the simplification of the equation in this section with the assumption that the experiment works on a vacuum/elastic-earth model rather than air/elastic-earth, and measurements are on the free surface (Figure 4).

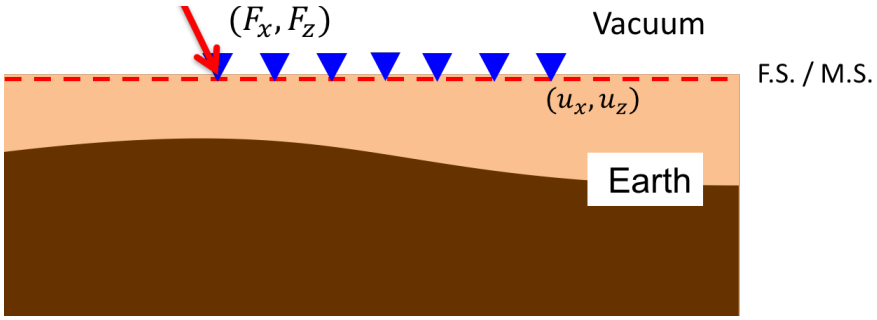

Figure 4: A vacuum/earth experiment at the free surface. Symbols same as the Figure 1.

With force equilibrium relationship,

$$\vec{t}(x', z' = 0, \omega) = -\vec{F}(\omega)\delta(x' - x_s)/\sqrt{1 + (dz'/dx')^2|_{x'=x_s}}, \tag{2}$$

where (x_s, z_s) is the source location, and $\sqrt{1 + (dz'/dx')^2|_{x'=x_s}}$ is a factor related to the shape of free surface at the source point. Substituted into Equation 1, the wave separation formula is transformed to be

$$\vec{u}^{up}(\vec{r}, \omega) = \vec{F}(\omega) \cdot \mathbf{G}_0(\vec{r}_s, \vec{r}, \omega) + \int_{m.s.} \vec{u}(\vec{r}', \omega) \cdot (\hat{n} \cdot \mathbf{\Sigma}_0(\vec{r}', \vec{r}, \omega))d\vec{r}', \tag{3}$$

The first integral in Equation 1 turns out to be a product, and only the Force information at the source point is required, which is an immediate data requirement reduction.

4 Traction computation at source point

The traction can be defined by

$$\vec{T} = \hat{n} \cdot \boldsymbol{\tau}, \tag{4}$$

where τ is the stress tensor. Considering an isotropic medium, and applying Hooke's law,

$$\boldsymbol{\tau} = \lambda \nabla \cdot \vec{u}\mathbf{I} + \mu(\nabla\vec{u} + \vec{u}\nabla), \tag{5}$$

where λ and μ are Lamé′s parameters of the elastic medium, and $\mathbf{I}$ is a unit dyadic.

The derivatives of the multicomponent displacements at the source points are required along both x- and z-directions to compute the traction there. The neighboring geophones can be used for the calculation of x-direction; whereas, an extra geophone below the source point can be used to measure displacement, and to facilitate the calculation of z-direction.

5 Numerical evaluation on a vacuum/earth model

To evaluate the simplified formula of Equation 3, we conduct three experiments, with different inputs as listed in Table 1. $\surd$ represents the input is available at all the receiver points. We expect the same result from the first two experiments, since the traction is always zero except at the source point for these experiments.

Experiment	Displacement	Traction
1	$\surd$	$\surd$
2	$\surd$	the force at source
3	$\surd$	none

Table 1: Inputs for the experiments and comparisons.

Layer's Number	P Velocity (m/s)	S Velocity (m/s)	Density (kg/m^3)
1	1000	500	1500
2	3000	1800	1800

Table 2: The parameters of the model in Figure 5.

Figure 5 describes the specific vacuum/earth model, with parameters shown in Table 2. All the source and receivers are on the free surface, which agree with the new formula's

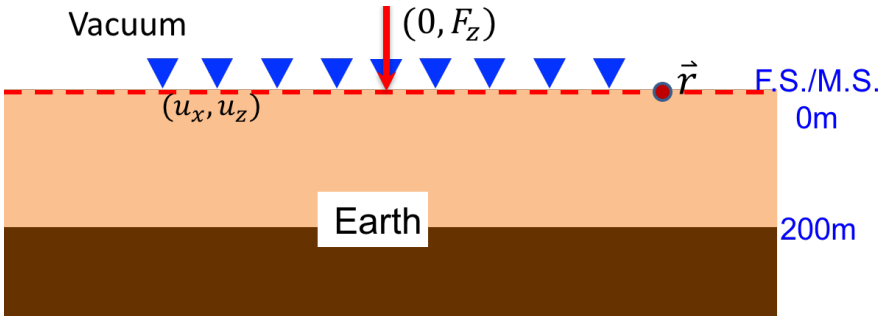

Figure 5: A two-layer vacuum/elastic-earth model for the numerical test. Symbol same as the Figure 1

assumption. The output point **r** is arranged on the measurement surface to be part of the volume above, by implementing the formula in the (k_x, ω) domain (see, e.g., Weglein et al. (2013)). With a vertical force as the excitation source, the term of product in Equation 3 equals to $(0, F_z * G_{zz})$ as one component of Green's tensor $G_{zx}(x_s, x, z_s = z = 0) = 0$. Thereby, the different inputs of traction can only affect the results of z component, but not x component.

With receivers at the free surface, the displacements (see Figure 6(a) for x component of total wave and Figure 7(a) for z component) display a strong Rayleigh waves and a relatively weak reflected waves. In addition, The interference between the ghosts and the upgoing waves starts at zero offset. Figure 6(b,c,d) show results of x component, with the three different traction inputs, which are tractions at all receiver points, corresponding force at the source point, and not available at all, respectively. All effectively predict the x component of upgoing waves, which agree with the previous analysis; i.e., for a vertical source experiment, the wave separation results along x direction are independent of traction. On the other hand, the first two experiments (Figure 7(b,c)) both produce satisfying results for z component. However, the third one (Figure 7(d)) that assumes the traction is zero everywhere leaves a strong residual, particularly for ground roll. The comparisons demonstrate that the force information at the source point is necessary and adequate to produce an accurate wave separation result.

6 Evaluation on an air/earth model

6.1 Problem description

The previous evaluation confirms the effectiveness of the modified wave-separation formula in removing both ground roll and ghosts, assuming a vacuum/elastic-earth model and a free-surface acquisition. However, the real world is better modeled as air/elastic-earth. A further evaluation of the reliability to solve a realistic problem using this new formula is necessary from a practical point of view; i.e., the usefulness of a vacuum/earth-interface assumption applying to an air/earth world should be examined.

6.2 Numerical evaluation

Another three experiments (defined in Table 1) are carried out, with parameters in Table 3. Both source and receivers are on the air/earth surface, and the output point is on the surface to be part of the volume above. Due to the reality that the traction is not zero at air/earth boundary, these three experiments lead to three different assumptions. The first one uses the traction everywhere along the measurement surface, assuming an air/earth model which is most accurate; the second one uses the force only at the source point, assuming a vacuum/earth model which is less accurate in comparison with the first experiment; the last one doesn't use traction at all, assuming traction is zero everywhere which is most inaccurate.

Layer's Number	P Velocity (m/s)	S Velocity (m/s)	Density (kg/m^3)
1	340	0	3
2	700	400	600
3	1500	800	1000

Table 3: The parameters of the air/earth model.

The results of onshore components can be seen in Figure 8(b,c,d). The first one (Figure 8(b)) produces the most accurate result; the second (Figure 8(c)) has a small residual for the ground roll at near offset; the last one (Figure 8(d)) shows a very strong residual. We select the traces at offset 400 m from Figure 8 (b,c,d) for a further comparison. The single-trace plot (in Figure 9) concludes that the separation result from the third experiment (in

Figure 8(d) and plotted by the black line in Figure 9) is not accurate; whereas the result from the second one (in Figure 8(c) and plotted by the blue line in Figure 9) is much closer to the first experiment (in Figure 8(b) and plotted by the red line in Figure 9), which is most accurate. We subtract the result from the second case and the third case with the first case, respectively. The absolute differences can be obtained trace by trace, and they are treated as the errors. The error analysis by averaging over all offsets shows that the second one (in Figure 8(c)) has an error of 4%, while the third (in Figure 8(d)) with 76%. The results of x component are not shown in this example, because the accurate results can be produced by all these experiments for a vertical force excitation.

7 Conclusion

The elastic Green's theorem based wave separation method has the potential to remove ground roll and ghosts for onshore exploration. The original algorithm demands both displacements and tractions. In this paper, we obtain a simplified formula that requires displacements along the surface but not traction anymore, as long as the force information at the source point or an approximate source wavelet information can be provided. The method assumes a vacuum/earth model and measurements performed at vacuum/earth surface. Although the new formula is derived under vacuum/earth-model assumption, the synthetic test indicates that it is still valuable for an air/earth model, which is closer to the real exploration environment.

8 Acknowledgements

We are grateful to all M-OSRP sponsors for encouragement and support in this research.

References

J. D. Mayhan and A. B. Weglein. First application of Green's theorem-derived source and receiver deghosting on deep-water Gulf of Mexico synthetic (SEAM) and field data. *Geophysics*, 78(2):WA77–WA89, 2013.

Y. H. Pao and V. Varatharajulu. Huygens principle, radiation conditions, and integral formulas for the scattering of elastic waves. *J. Acoust. Soc. Am.*, 59:1361–1371, 1976.

L. Tang, J. D. Mayhan, J. Yang, and A. B. Weglein. Using Green's theorem to satisfy data requirements of multiple removal methods: The impact of acquisition design. *83rd Annual International Meeting, SEG, Expanded Abstracts*, pages 4392–4396, 2013.

A. B. Weglein and B. G. Secrest. Wavelet estimation for a multidimensional acoustic earth model. *Geophysics*, 55(7):902–913, 1990.

A. B. Weglein, S. .A. Shaw, K. H. Matson, J. L. Sheiman, R. H. Solt, T. H. Tan, A. Osen, G. P. Correa, K. A. Innanen, Z. Guo, and J. Zhang. New approaches to deghosting towed-streamer and ocean-bottom pressure measurements. *72th Annual International Meeting, SEG, Expanded Abstracts*, pages 1016–1019, 2002.

A. B. Weglein, J.D. Mayhan, L. Amundsen, H. Liang, J. Wu, L. Tang, Y. Luo, and Q. Fu. Green's theorem deghosting algorithms in (k, ω) as a special case of (x, ω) algorithms. *Journal of Seismic Exploration*, 22:389–412, 2013.

J. Wu and A. B. Weglein. Elastic Green's theorem preprocessing for on-shore internal multiple attenuation: theory and initial synthetic data tests. *84th Annual International Meeting, SEG, Expanded Abstracts*, pages 4299–4304, 2014.

J. Wu and A. B. Weglein. Preprocessing in displacement space for on-shore seismic processing: removing ground roll and ghosts without damaging the reflection data. *85th Annual International Meeting, SEG, Expanded Abstracts*, pages 4626–4630, 2015a.

J. Wu and A. B. Weglein. Preprocessing in PS space for on-shore seismic processing: removing ground roll and ghosts without damaging the reflection data. *85th Annual International Meeting, SEG, Expanded Abstracts*, pages 4740–4744, 2015b.

J. Yang, J. D. Mayhan, L. Tang, and A. B. Weglein. Accommodating the source (and receiver) array in free-surface multiple elimination algorithm: Impact on interfering or proximal primaries and multiples. *83rd Annual International Meeting, SEG, Expanded Abstracts*, pages 4184–4189, 2013.

Öz Yilmaz. *Seismic Data Analysis: Processing, inversion and Interpretation of Seismic Data*. Society of Exploration Geophysicists, 2001.

J. Zhang. *Wave theory based data preparation for inverse scattering multiple removal, depth imaging and parameter estimation: analysis and numerical tests of Green's theorem deghosting theory*. PhD thesis, University of Houston, 2007.

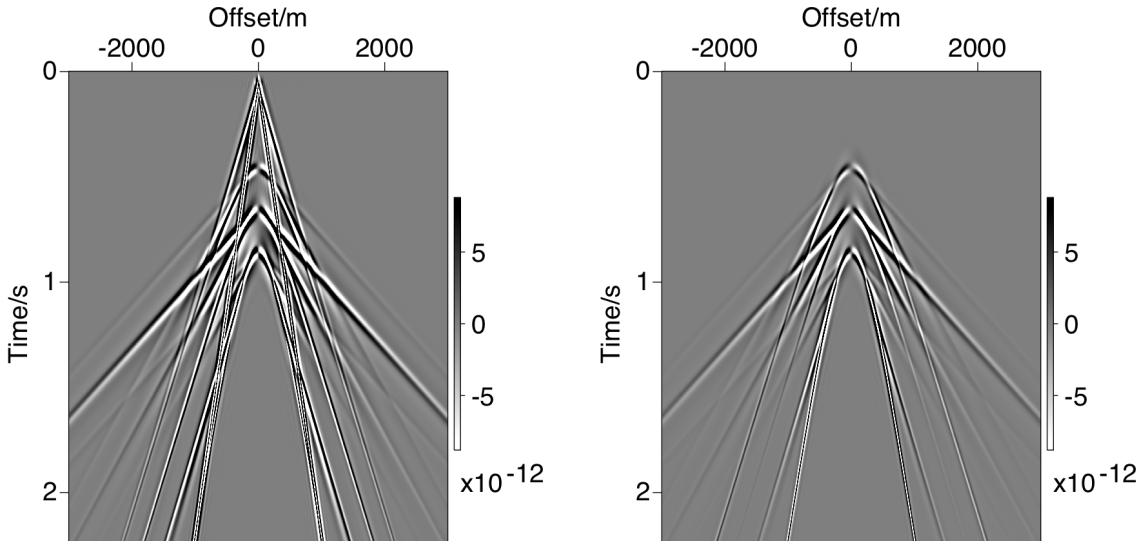

(a) u_x

(b) u_x^{up1}

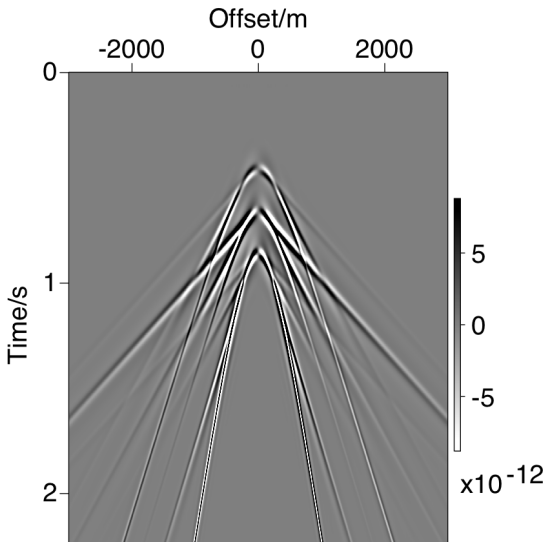

(c) u_x^{up2}

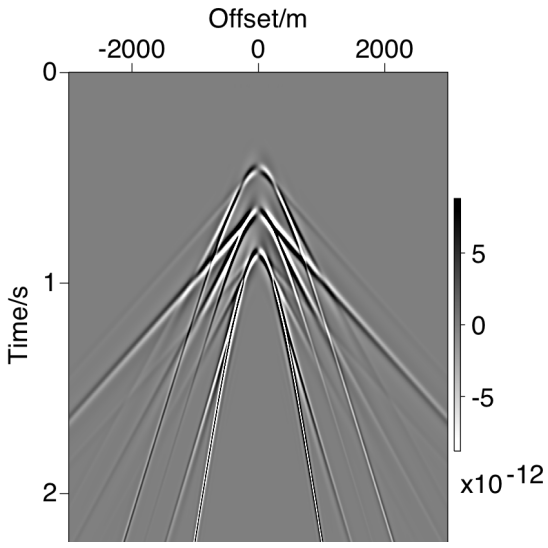

(d) u_x^{up3}

Figure 6: Wave separation on vacuum/earth model. (a) for x component total wave; (b) for x component separated up wave from case 1; (c) for x component result from case 2; (d) for x component result from case 3.

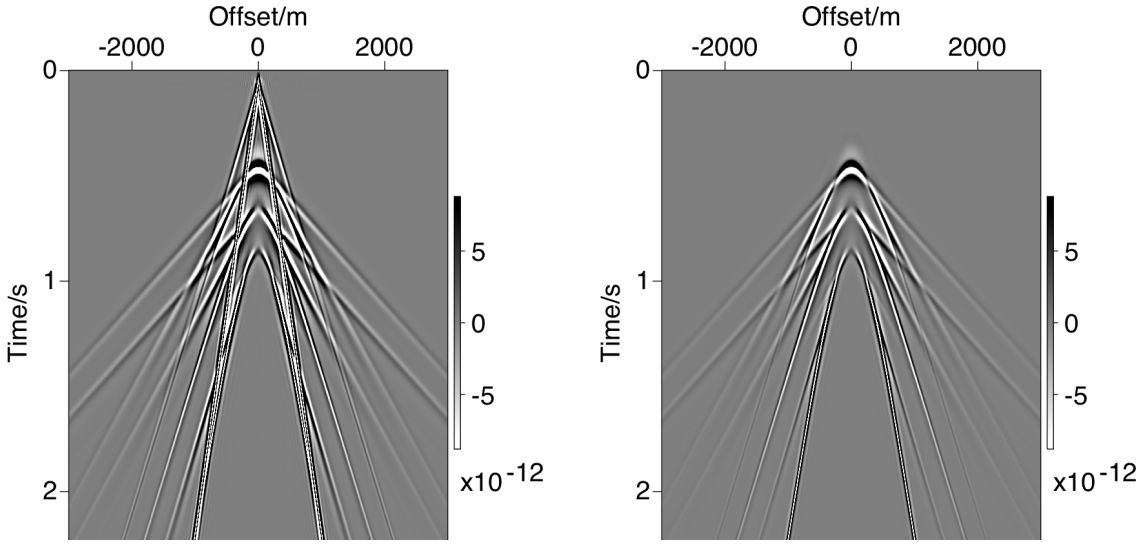

(a) u_z

(b) u_z^{up1}

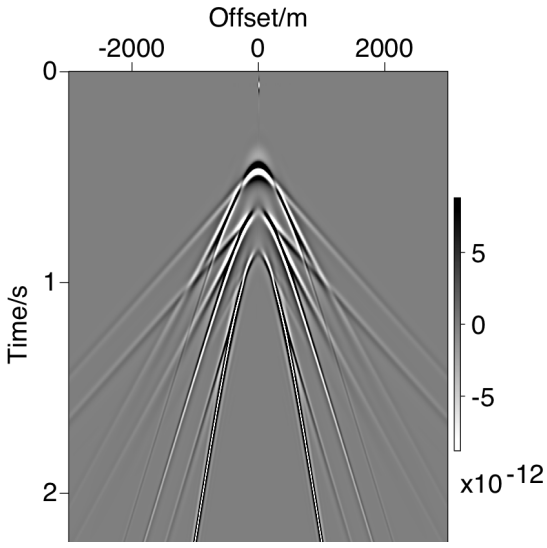

(c) u_z^{up2}

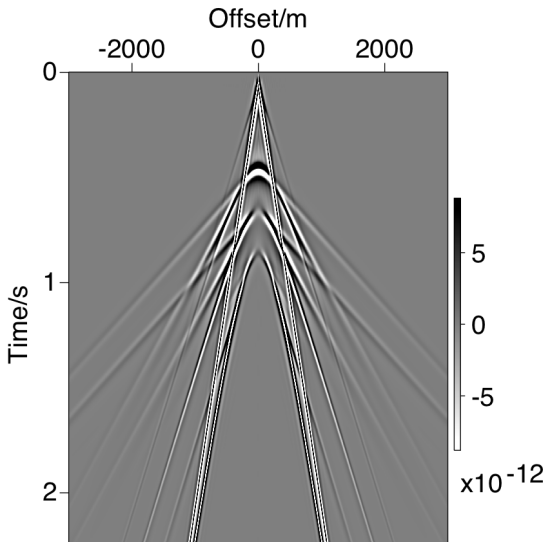

(d) u_z^{up3}

Figure 7: Wave separation on vacuum/earth model for z component. (a) for z component total wave; (b) for z component separated up wave from case 1; (c) for z component result from case 2; (d) for z component result from case 3.

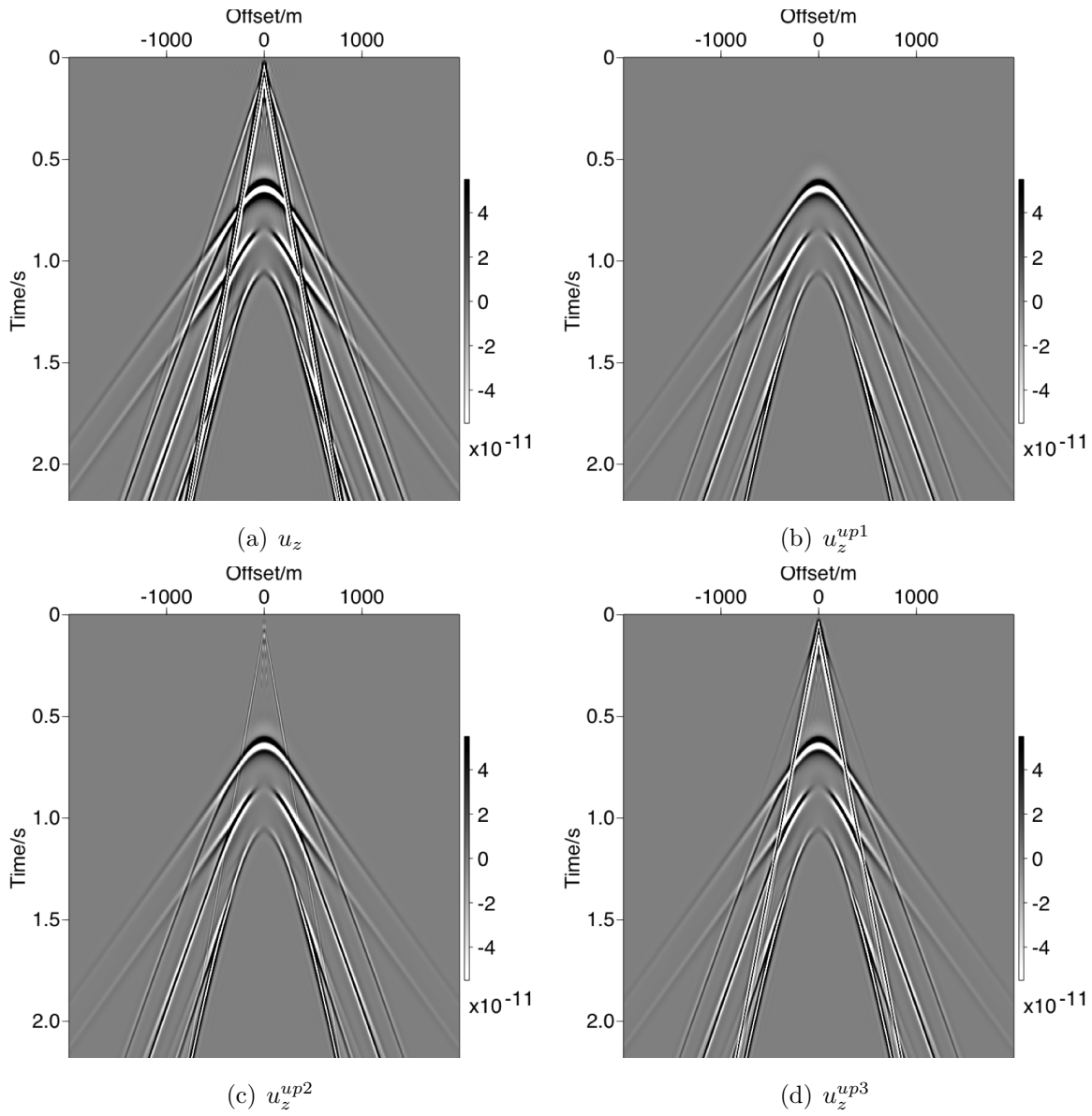

(a) u_z

(b) u_z^{up1}

(c) u_z^{up2}

(d) u_z^{up3}

Figure 8: Wave separation on air/earth model for z component. (a) for total wave; (b) for separated up wave from case 1; (c) for the result from case 2; (d) for the result from case 3.

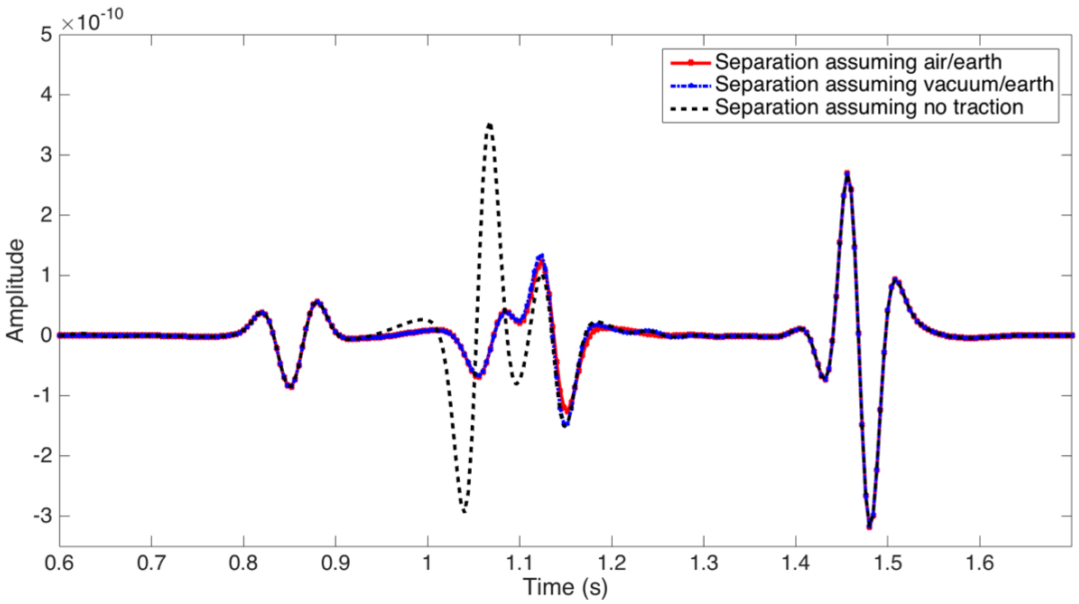

Figure 9: Single trace comparison at offset 400 m, extracting from the wave separation results plotted in Figure 8 (b,c,d).